Jaydeep Karandikar
Georgia Institute of Technology,
Atlanta, GA 30332
e-mail: jaydeep.karandikar@me.gatech.edu

Michael Traverso
Stanford University,
Stanford, CA 94305
e-mail: miketrav@stanford.edu

Ali Abbas
University of Illinois at Urbana-Champaign,
Urbana, IL 61801
e-mail: aliabbas@illinois.edu

Tony Schmitz
University of North Carolina at Charlotte,
Charlotte, NC 28223
e-mail: tony.schmitz@uncc.edu

Bayesian Inference for Milling Stability Using a Random Walk Approach

Unstable cutting conditions limit the profitability in milling. While analytical and numerical approaches for estimating the limiting axial depth of cut as a function of spindle speed are available, they are generally deterministic in nature. Because uncertainty inherently exists, a Bayesian approach that uses a random walk strategy for establishing a stability model is implemented in this work. The stability boundary is modeled using random walks. The probability of the random walk being the true stability limit is then updated using experimental results. The stability test points are identified using a value of information method. Bayesian inference offers several advantages including the incorporation of uncertainty in the model using a probability distribution (rather than deterministic value), updating the probability distribution using new experimental results, and selecting the experiments such that the expected value added by performing the experiment is maximized. Validation of the Bayesian approach is presented. The experimental results show a convergence to the optimum machining parameters for milling a pocket without prior knowledge of the system dynamics. [DOI: 10.1115/1.4027226]

1 Introduction

Discrete part production by machining is an important manufacturing capability in many industries. Limitations to milling productivity include tool wear, positioning errors of the tool relative to the part, spindle error motions, fixturing concerns, programming challenges, and the instability introduced by the process dynamics. Improved high-speed machining technology has made increased spindle speeds and axial depths of cut possible. The foundation for much of this work can be traced to papers by Tlusty and Polacek [1], Tobias and Fishwick [2], and Merrit [3], which, in turn, followed earlier work by Arnold [4] and others. Based on these efforts, an understanding of the regeneration of surface waviness during material removal as a primary mechanism for chatter in machining was established. When combined with the effects of forced vibrations during stable cutting, the basis for exploring the role of machining dynamics in discrete part production is established. Comprehensive reviews of subsequent modeling and experimental efforts have been compiled and presented in the literature (e.g., Refs. [3] and [5–12]).

Although milling models are typically treated as deterministic, it is often observed in practice that stable points may lie above or below the predicted stability boundary. This is due to inaccuracy in the measured/modeled structural dynamics [13,14], cutting force coefficients, and stability model approximations. Existing stability formulations typically do not incorporate uncertainty effects, although some previous work has been done [15]. Furthermore, although methods are available for predicting the spindle speed-dependent stability limit, the requirement for knowledge of the tool point frequency response function (for each tool-holder-spindle-machine combination) can impose a significant obstacle in some production facilities.

In this study, the authors implement the normative foundations of decision theory to not only enable a probabilistic characterization of the stability boundary but also provide a systematic method to select pre-machining experiments and quantify their value. As a first step toward the goal of probabilistic stability modeling, a simple "model," or initial belief, is applied that does not require knowledge of the system dynamics or cutting force coefficients. The goal of the study is to converge to the optimum machining parameters for milling a pocket by experimentation at machining parameters which add the most value to expected profit.

2 Bayesian Inference

Bayesian inference provides a normative and rational method for belief updating when new information in the form of experimental results is made available. Let the prior distribution about an uncertain event, A, at a state of information, &, be $\{A|\&\}$, the likelihood of obtaining an experimental result B given that event A occurred be $\{B|A,\&\}$, and the probability of receiving experimental result B (without knowing A has occurred) be $\{B|\&\}$. Bayes' rule determines the posterior belief about event A after observing the experiment results, $\{A|B,\&\}$ as shown in Eq. (1). Using Bayes' rule, information gained through experiments can be incorporated with the prior prediction about the stability limit to obtain a posterior distribution,

$$\{A|B,\&\} = \frac{\{A|\&\}\{B|A,\&\}}{\{B|\&\}} \tag{1}$$

For milling stability, the uncertainty that exists in the true limiting axial depth for each spindle speed is modeled using a probability distribution over a set of all possible stability limits. The probability distribution is then updated using experimental results and Bayes' rule (Eq. (1)). Using Bayesian inference, the predictive model incorporates uncertainty and updates beliefs as new information is made available (from experiments, for example). An important step in applying Bayes' rule is establishing the initial belief, or prior, for the stability limit. In general, this initial prediction: (1) can be constructed from any combination of theoretical considerations, previous experimental results, and expert opinions and (2) should be chosen to be as informative as possible regarding the experimenter's belief. In this study, the prior is determined assuming no knowledge of the system dynamics; it is based on the assumption that it is more likely to get an unstable cut as the axial depth is increased for any spindle speed. This simple prior probability distribution of stability is then updated using experimental results.

Contributed by the Manufacturing Engineering Division of ASME for publication in the Journal of Manufacturing Science and Engineering. Manuscript received July 29, 2011; final manuscript received February 17, 2014; published online April 11, 2014. Assoc. Editor: Suhas Joshi.

Bayesian inference offers several advantages. First, it takes into account the inherent uncertainty in the model by using a probability distribution. Second, the uncertainty (i.e., the probability distribution) can be updated using experimental data. Third, the combination of Bayesian inference and decision theory enables experiments to be selected such that the expected value added by performing the experiment is maximized, which enables the best selection of experiments. The remainder of the paper is organized as follows. Section 3 describes the Bayesian updating for milling stability using a random walk approach. Section 4 describes the selection of experimental tests points using the value of information approach. The experimental results and validation are presented in Sec. 5. Section 6 details additional considerations when using the proposed method.

3 Bayesian Updating of Milling Stability

Bayesian inference provides a rigorous mathematical framework for updating belief about an uncertain variable when new information becomes available. The prior belief is captured using a probability distribution for the variable of interest, where the prior probability distribution about the location of the stability boundary in milling, expressed as a function of spindle speed and axial depth, is assigned by the user. In the case of milling, a joint probability distribution characterizing the probability of stability for all axial depths, b, and spindle speeds, Ω, is required. Since there is a continuum of axial depths and spindle speeds, it is helpful to use some structure in defining the joint distribution. The structure used here incorporates a random walk methodology with a Markov structure. A Markov structure means that the conditional probability assignment to any future state depends only on the present state and not on the past states.

3.1 Random Walk Methodology. A random walk can be described as the probabilistic path, where the change in position at each time increment depends on the current position but is independent of all the past positions of the path. A random walk with a normally distributed step size in the particle position, x, is used in this study. This normally distributed step size in x states that the change in position at any time is a random value selected from a normal distribution.

To illustrate, let the initial position of x be zero at time $t = 0$. At the next time instant, t_1, the new position of x is sampled from the normal distribution, $N(\mu,\sigma)$, with a mean of μ and standard deviation of σ. Subsequently, the position of x at any arbitrary time, t_i, is the sum of the previous position and a random value,

$$x(t = t_i) = x(t = t_i - 1) + N(\mu, \sigma) \tag{2}$$

Note that the value at any future state depends only on the present state, but not on any of the previous states. Figure 1 (left) shows 20 sample paths of x starting at $t = 0$ s and continuing to $t = 10$ s. The time axis was divided into discrete increments of 0.01 s and the new position was sampled for each of these increments. The position step size was normally distributed with zero mean and standard deviation equal to 0.1, i.e., $N(0,0.1)$. At each time increment of 0.01 s, the position of x was determined by the addition of its current position and a randomly generated x step size sampled from $N(0,0.1)$. Thus, $x(t = t_i) = x(t_i - 0.01) + N(0,0.1)$. A normally distributed step size ensures that the distribution of x at any time instant is also normal. Additionally, since the step size distribution has zero mean, the mean of the distribution of x is nominally zero at all time instants. Figure 1 (right) shows 5000 sample paths generated using $N(0,0.1)$, starting from $x = 0$ at $t = 0$ s. Figure 2 shows the distribution of x at $t = 5$ s (left) and $t = 10$ s (right). As shown in the figure, the distribution of x is normal with a zero mean. It is also observed that the variance increases with time. Since the increments are generated independently, the variance after n steps is equal to the variance of each increment multiplied by n. Comparing the two distributions in Fig. 2 shows that the uncertainty in x increases with time.

3.2 Bayesian Inference. The random walk method can be applied to describe the prior belief about the uncertain stability boundary (or limit) in a spindle speed-axial depth of cut domain given knowledge of the limit at a particular point in the domain. The sample paths can be generated in spindle speed increments (instead of time) and the position step size is selected for the axial depth of cut. The stability boundary prediction proceeds by generating N sample paths, each of which may represent the actual stability boundary. The probability that each sample path is the true stability limit based on this model is $1/N$. These sample paths are used as the prior in applying Bayesian inference. This prior shows that the uncertainty in the location of the stability limit increases when moving further away from a point (i.e., a combination of spindle speed and axial depth) where the stability limit is known. The prior probability is then updated by experimental results using Bayes' rule. For each sample path, Bayes' rule can be written as

$$\begin{aligned} &P(\text{path} = \text{true stability limit} \mid \text{testresult}) \\ &\quad \propto P(\text{test result} \mid \text{path = true stability limit}) \\ &\quad \times P(\text{path} = \text{true stability limit}) \end{aligned} \tag{3}$$

Here, $P(\text{path} = \text{true stability limit})$ is the prior probability which, before any testing, is equal to $1/N$ for any sample path and $P(\text{test result} \mid \text{path} = \text{true stability limit})$ is the likelihood of obtaining the

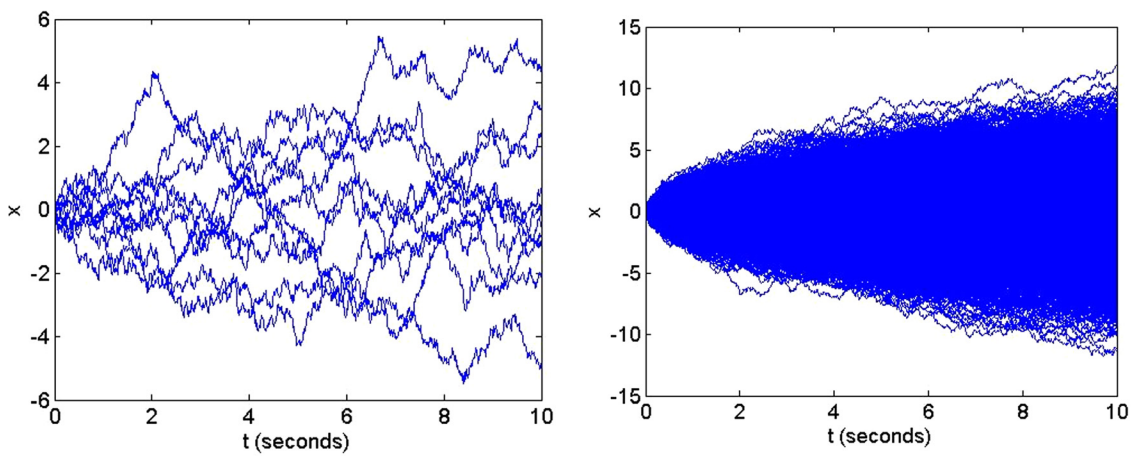

Fig. 1 Twenty (left) and 5000 (right) random walks with a normally distributed position step size described by $N(0,0.1)$

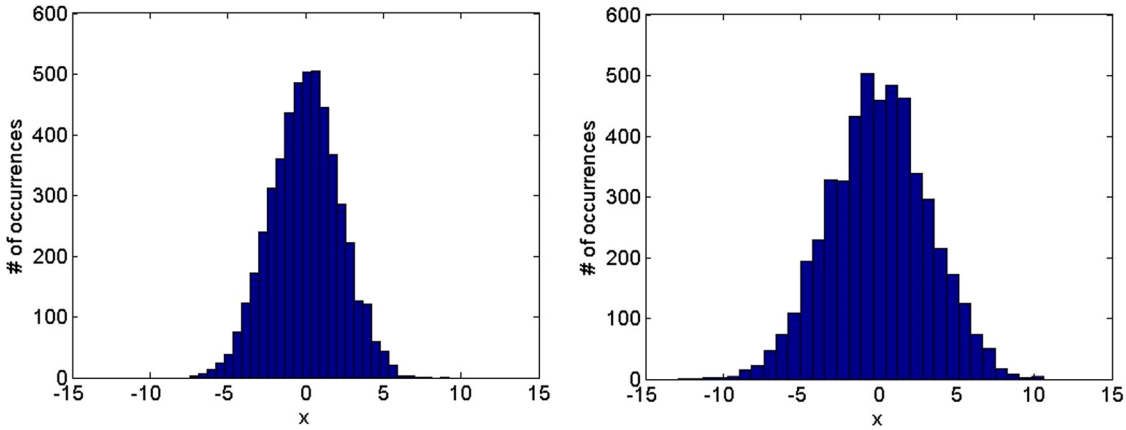

Fig. 2 Histograms of *x* at 5 s (left) and 10 s (right)

test result given the true stability limit. Their products yield the posterior stability limit probability given the test result, P(path = true stability limit | test result). In practice, the probability of the test result, P(test result), may be used to normalize the posterior probability (by dividing the right hand side of Eq. (3) by this value).

3.3 Constructing the Prior Distribution. In Bayesian inference, the prior probability represents the initial degree of belief regarding the stability limit. The sample paths generated using the random walks are used to define a prior probability of stability. To construct the prior, a spindle speed-axial depth of cut domain was first defined. For demonstration purposes, the operating spindle speed was arbitrarily selected to be between 4000 rpm and 10,000 rpm. It was assumed that for all spindle speeds within the operating range, the stability limit is between 0 and the maximal axial depth defined by the flute length (selected to be 10 mm). Following the same procedure described in Sec. 3.1, random walks were generated. The starting point was the midpoint of the axial depth range (5 mm). The sample paths were started from $\Omega = 0$ rpm to allow the paths to cross the maximum axial depth of 10 mm by 4000 rpm and continued to $\Omega = 15{,}000$ rpm. The step size in mm was described by $N(0,0.5)$. Figure 3 shows many sample paths.

Each sample path represents the true stability limit with some probability. To illustrate how we can incorporate our prior information this way, suppose we would like to confine the stability limit within the spindle speed range 4000 rpm and 10,000 rpm to be between within the axial depths 0 and 10 mm. This implies that the paths which cross outside 0 or 10 mm within the spindle speed range of 4000 rpm to 10,000 rpm have a zero probability of being the true stability limit since they are outside the pre-defined stability domain. These sample paths are filtered out or multiplied by zero. The probability that the remaining paths represent the true stability limit is now $1/N$, where N is the number of remaining paths. Figure 4 shows 10,000 sample paths which have the axial depth within 0–10 mm in the spindle speed range of 4000 rpm to 10,000 rpm.

Figure 5 shows the histogram of axial depths at 4000 rpm at 10,000 rpm. Note that the axial depth histograms are confined within 0 mm and 10 mm due to path filtering. The mean is 5 mm at all spindle speeds since the starting point of the walks was selected as 5 mm.

The excess cumulative distribution function (cdf) is then calculated at each spindle speed within the domain using the histograms. The excess cdf gives the probability that an axial depth will be stable. Figure 6 (left) shows the excess cdf over the spindle speed domain. Figure 6 (right) shows the excess cdf for the axial depth, which is initially the same at each spindle speed. As shown in Fig. 6, the probability is 0 that an axial depth greater than 10 mm will be stable and the probability that an axial depth greater than 5 mm will be stable is 0.5. The cdf therefore states that the probability of obtaining a stable cut increases as the axial depth of cut is reduced. Since machining is not possible at an axial depth of 0, the minimum axial depth is taken to be 0.01 mm. It represents the prior or initial belief, about the stability boundary. In this case, the prior was only based on the assumption that the probability of obtaining a stable cut decreases with higher axial depths.

3.4 Updating Using Experimental Stability Results. In the case of stability testing, if the true stability limit was known, then

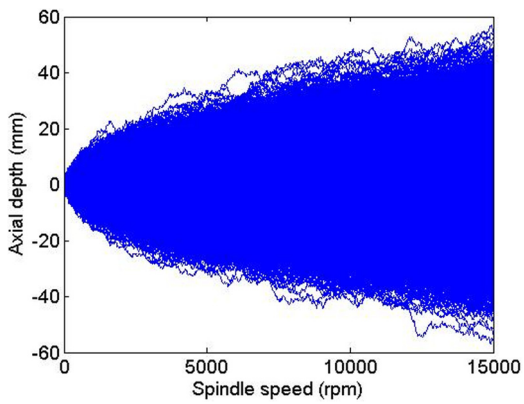

Fig. 3 Many sample paths generated in the spindle speed-axial depth domain

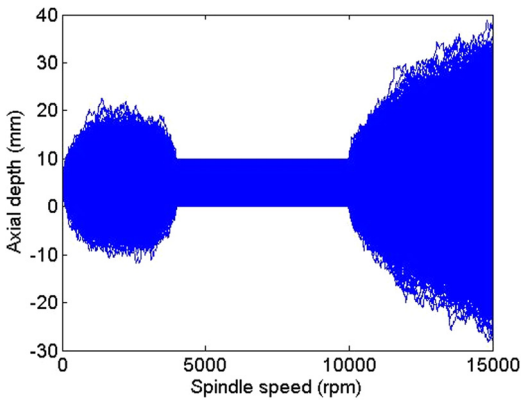

Fig 4 10,000 sample paths after filtering. The paths that cross 0 or 10 mm in the spindle speed range of 4000 rpm to 10,000 rpm have been removed.

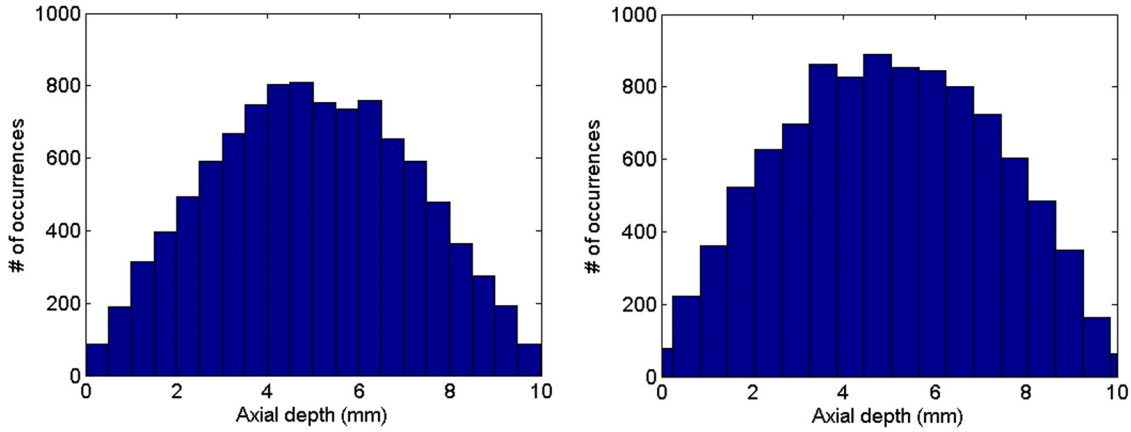

Fig. 5 Histograms of axial depths at 4000 rpm (left) and 10,000 rpm (right)

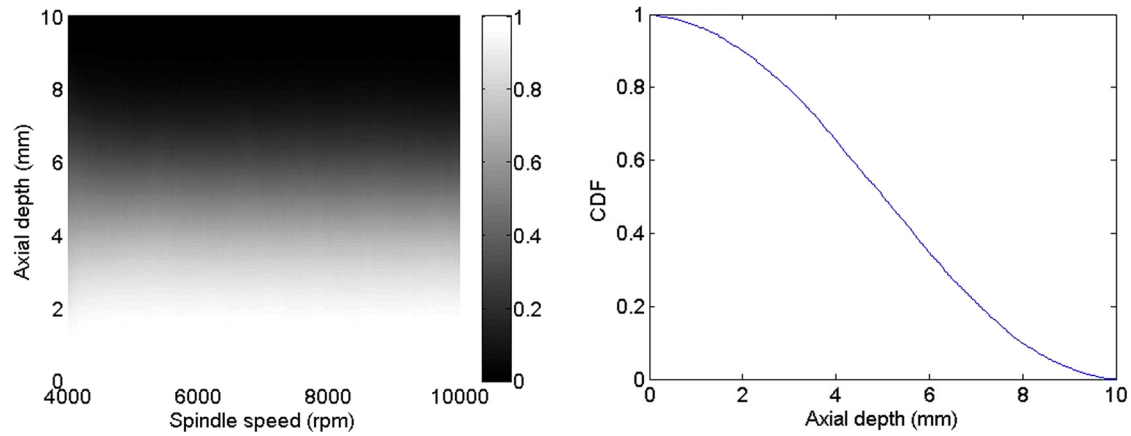

Fig. 6 Prior probability of stability in the spindle speed-axial depth domain (left). The probability of stability is 0 at an axial depth of 10 mm.

it would be known with certainty whether the result of a test would be stable or unstable. The test would be stable with a probability of 1 if the test point was below the stability limit and stable with a probability of 0 (unstable with a probability of 1) if the test point was above the stability limit. For the random walk approach, recall that each sample path represents the true stability limit with a probability of $1/N$. Suppose a test is performed at some spindle speed-axial depth combination and the result is stable. This implies that all paths that with axial depths below the test point at the selected spindle speed cannot be the true stability limit (according to linear stability theory and the traditional Hopf bifurcation behavior [1–3,16]). Similarly, for an unstable test result, all paths with a higher axial depth at the test spindle speed cannot be the true stability limit. Therefore, for a stable test, the likelihood for each path which with a higher axial depth than the test point is 1 and the likelihood for each path with a lower axial depth is 0. Similarly, for an unstable test, the likelihood for each path with a higher axial depth is 0 and the likelihood for each path with a lower axial depth than the test point is 1.

Because the likelihood for every path is always either 0 or 1, the updating procedure proceeds by filtering out paths after each test result. After any number of tests, all paths which have not been filtered out (i.e., multiplied by a likelihood of 0) will have a probability equal to the reciprocal of the remaining number of paths. When updating the prior using a test result, the paths which do not agree with the test result are filtered out and the remaining paths represent the updated stability prediction.

To illustrate, consider a stability test completed at $\Omega = 7000$ rpm and $b = 5$ mm. A stable test implies that all axial depths below 5 mm would be stable at $\Omega = 7000$ rpm. As a result, the likelihood that any path that with an axial depth less than 5 mm at $\Omega = 7000$ rpm is the true stability limit is zero. All such paths are filtered out, or multiplied by zero, to obtain the updated prediction. Similarly, if the test at $\Omega = 7000$ rpm and $b = 5$ mm was unstable, the likelihood that any path with an axial depth greater than 5 mm at $\Omega = 7000$ rpm is the true stability limit is zero and all such paths are filtered out. Figure 7 shows the remaining paths after filtering given a stable test result (left) and an unstable test result (right). As seen in Fig. 7, all paths that are below 5 mm at 7000 rpm are filtered out for a stable test result while the paths above 5 mm at 7000 rpm are filtered out for an unstable test result. Note that Fig. 7 only shows the path in the spindle speed range from 4000 rpm to 10,000 rpm.

The updated probability distributions can then be calculated using the data from the histograms of axial depths at each spindle speed within the domain. As noted, all paths which have not been filtered out (those with a likelihood of 1) will have a probability equal to the reciprocal of the remaining number of paths. For a stable result at $\Omega = 7000$ rpm and $b = 5$ mm, the remaining number of paths is 4970 while an unstable result gives 5030 remaining paths for this example. Figure 8 shows the updated excess cdf at the test speed given a stable result (left) and an unstable result (right). Figure 9 shows the updated posterior cdf of stability given a stable (left) and unstable (right) result at $\Omega = 7000$ rpm and $b = 5$ mm. As seen from the posterior cdf, the single test updates the distribution at all spindle speeds. The extent to which a test at one spindle speed updates the distribution at all speeds depends on the standard deviation of the step size for the random walk. This dependence is evaluated in Sec. 6.

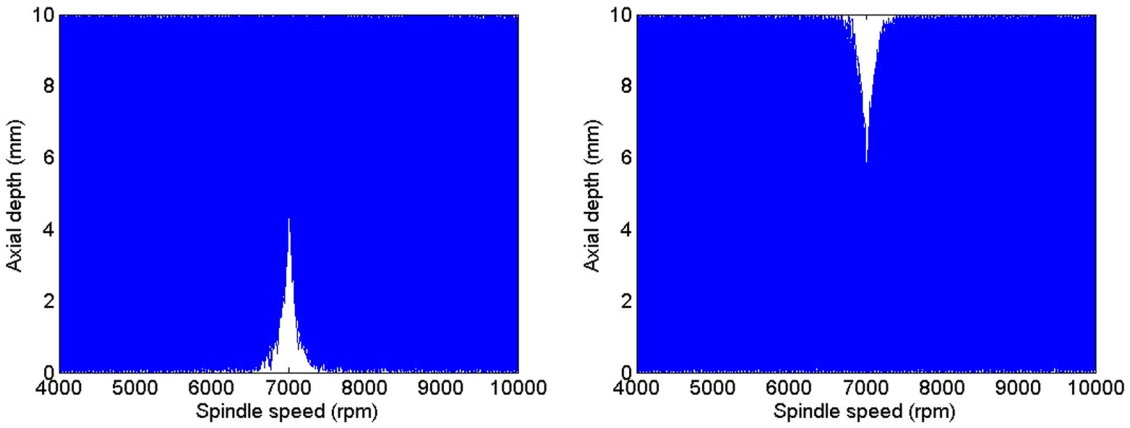

Fig. 7 Sample paths remaining after filtering given a stable test result (left) and an unstable test result (right) at and axial depth of 5 mm and spindle speed of 7000 rpm

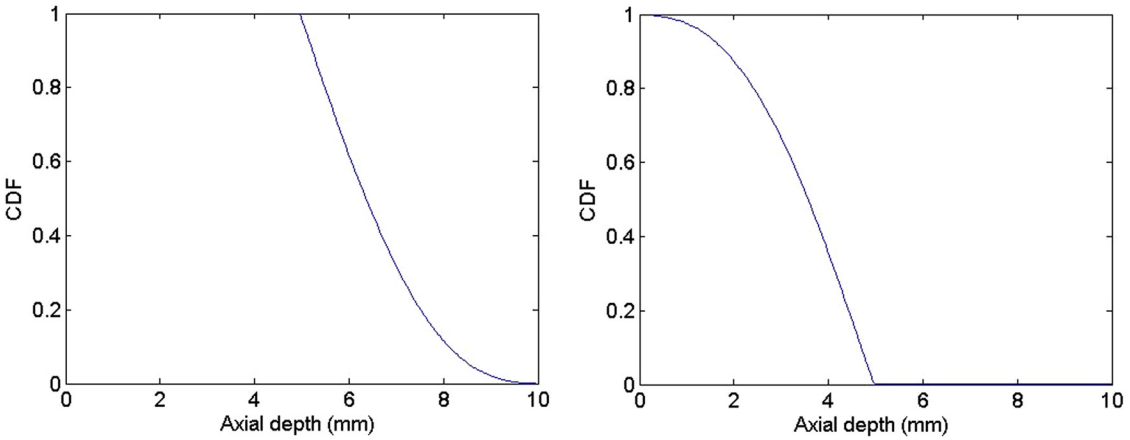

Fig. 8 Updated cdf at 7000 rpm given a stable test result (left) and an unstable test result (right) at a test axial depth of 5 mm

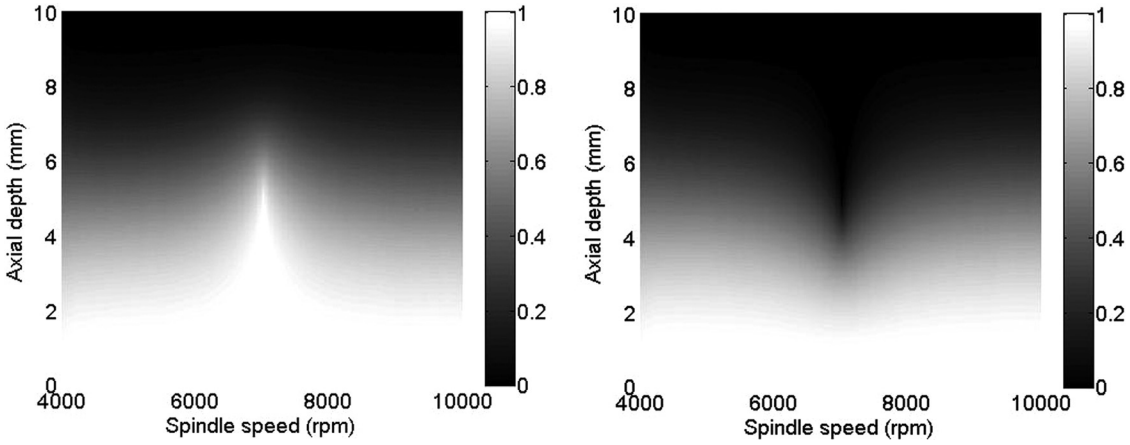

Fig. 9 Posterior cdf for milling stability given a stable test result (left) and an unstable test result (right) at an axial depth of 5 mm and spindle speed of 7000 rpm

4 Value of Information for Experiment Selection

Bayesian inference combined with decision analysis models enables a dollar value to be placed on the information gained from an experiment prior to performing it. This value is referred to as the *value of information* [17,18]. It may be defined as the expected profit before testing minus the profit after testing or, in terms of cost, the expected cost prior to testing minus the cost after testing [17]. Note that while the value of information uses expected value after testing, it is calculated before actually performing the test.

The primary motivation for defining the value of information is to optimize the selection of experiments. The experimental test point is selected which adds the most (expected) value to the profit. In addition, if the expected cost of performing an experiment is more than the expected value gained from the experiment, it is not recommended that the experiment be completed. This is a

major advantage over statistical design of experiments, which typically does not consider profit in test point selection. In the value of information approach to milling stability modeling, a test is performed at a point where the maximum information/value about the stability limit is obtained.

To illustrate this point, consider a simple situation where only three spindle speed-axial depth combinations are available (A, B, and C). Suppose it is initially predicted that A is definitely stable, while B and C each have a 50% chance of being stable. In addition, suppose that the cost of machining (assuming the cut is stable) is \$100 using A, \$50 using B, and \$30 using C and that only stable operating points will be used (based on the assumption that the cost of performing an unstable cut is very large due to the subsequent rework or scrap). Prior to performing the stability test, only A can be chosen as the operating point and, therefore, if no testing is performed the cost of machining will be \$100. However, suppose the option of performing a single stability test at either A, B, or C was given. How can the proper test be selected? Because it is already known that a test at A will have a stable result, no test should be completed at A because no new information will be obtained. However, if it was possible to test at B, there is a 50% chance that the result is unstable, in which case the choice will still be A and the cost will be \$100. On the other hand, there is also a 50% chance that the test will be stable, in which case B will be selected and the cost will only be \$50. The expected cost of machining given the result of a test at B is therefore \$75. The value gained by testing at B (defined as the cost prior to testing minus the expected cost after testing) is \$25. Similarly, the value gained by testing at C can also be calculated. There is a 50% chance that the result will be unstable, in which case machining will be completed at A and the cost will be \$100. There is also a 50% chance that the test will be stable and then machining will be completed at C and the cost is only \$30. Thus, the expected cost given the result of a test at C is \$65 and the value gained by testing at C is \$35. Now (assuming the goal is to maximize profit), the question of which test to perform has a straightforward answer: choose the test which adds the most value. For this example, testing would be completed at C.

4.1 Cost Formulation. Before calculating the value of information, it is necessary to determine the cost of performing the operation given the selected operating conditions. To calculate the cost, a the feature to be machined was specified as a pocket with dimensions of 150 mm in the x direction, 100 mm in the y direction, and 25 mm deep. The tool path is shown in Fig. 10.

The cost function does not include the effects of tool wear; it was neglected for the 6061-T6 workpiece/TiCN-coated carbide tool combination considered in this study. The simplified cost, C, shown in Eq. (3) is based on the machining cost per minute, $r_m = \$2$, and machining time, t_m, which depends on the part path geometry and machining parameters. The parameters used to calculate the cost for machining the pocket are listed in Table 1. Due to the nature of the part path, for any selected spindle speed the cost function is stepped (see Fig. 11). These steps occur at an integer fraction of the pocket depth

$$C = r_m t_m \tag{4}$$

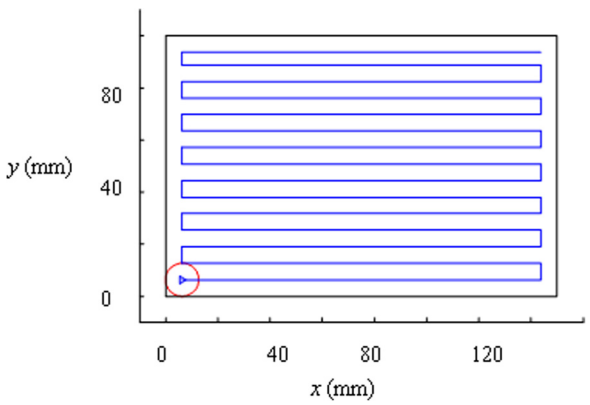

Fig. 10 Tool path for pocket milling

Table 1 Parameters used to determine the reference stability limit for the simulated testing scenario

Parameter	Value	Units
Radial depth	19.0	mm
Feed per tooth	0.06	mm/tooth
Tool radius	9.5	mm
Number of teeth	1	teeth
Helix angle	0	deg

4.2 Selecting the Test Points. The revenue generated by machining the selected pocket is assumed to be \$2000 for this example. Profit is defined as the revenue generated minus the machining cost. For constant revenue (generated in machining the feature), maximizing profit is equivalent to minimizing the expected cost. Since each point has a probability of stability, the expected profit a given pair of operating parameters, $\{\Omega_{op}, b_{op}\}$, is given by

$$V_{prior}\{\Omega_{op}, b_{op}\} = P_{stable}\{\Omega_{op}, b_{op}\}V_{stable}\{\Omega_{op}, b_{op}\} + (1 - P_{stable}\{\Omega_{op}, b_{op}\})V_{unstable}\{\Omega_{op}, b_{op}\} \tag{5}$$

where the subscript "op" denotes operating point, P_{stable} is the random walk prior probability of stability at the operating point (see Fig. 6), V_{stable} is the profit given that the cut is stable, $V_{unstable}$ is the profit given that the cut is unstable, and V_{prior} is the expected profit for machining the pocket at $\{\Omega_{op}, b_{op}\}$ prior to performing any further test. Unstable operating points are considered infeasible, since it is assumed that the cost added by reworking the part and the cost associated with potential damage to tooling are substantially higher than the revenue generated in machining the pocket. Thus, the operating point would be the one which is stable with certainty ($P_{stable} = 1$) and provides the highest profit within the domain (according to Eq. (5)). This implies that the cost of instability is negative infinity. Recall that it was assumed that a 0.01 mm axial depth is stable at all spindle speeds within the domain. Therefore, before performing any test, the profit would be

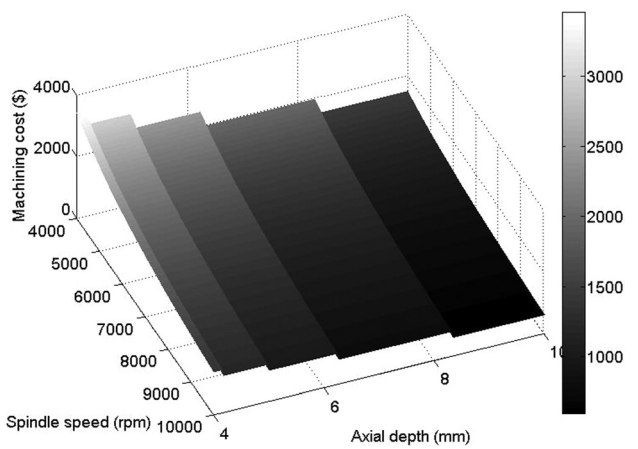

Fig. 11 Cost of machining at axial depth–spindle speed combinations given that the resultant cut is stable. Notice the steps in the cost function at integer fractions of the pocket depth.

highest at an axial depth of 0.01 mm and spindle speed of 10,000 rpm since the machining time would be minimized at the maximum spindle speed. The maximum profit before performing any test, V^*_{prior}, is therefore the profit at {10,000, 0.01}.

The expected value of performing a test at any point $\{\Omega_{\text{test}}, b_{\text{test}}\}$ is calculated as follows (the subscript *test* indicates a test point). Each test is assumed to be either stable or unstable. The resultant posterior cdf is different for a stable result at the test point than it is for an unstable result (see Fig. 9). Subsequently, the profit after the test, calculated using the posterior cdf, is also different for a stable test than for an unstable test. Assume that a test at $\{\Omega_{\text{test}}, b_{\text{test}}\}$ is stable. The maximum profit would be at $\{\Omega_{\text{test}}, b_{\text{test}}\}$, since that operating point is known to be stable with certainty. The maximum profit would be equal to $V_{\text{stable}}\{\Omega_{\text{test}}, b_{\text{test}}\}$. However, if the cut is unstable, the maximum expected profit would be equal to the maximum profit before performing the test, V^*_{prior}. This is the case because with an unstable test cut, no additional point is known to be stable with certainty and the cost of an unstable cut is negative infinity. Thus, the expected profit, V_{test}, after performing a test at any $\{\Omega_{\text{test}}, b_{\text{test}}\}$ is given by

$$V_{\text{test}}\{\Omega_{\text{test}}, b_{\text{test}}\} = P_{\text{stable}}\{\Omega_{\text{test}}, b_{\text{test}}\}V_{\text{stable}}\{\Omega_{\text{test}}, b_{\text{test}}\} + (1 - P_{\text{stable}}\{\Omega_{\text{test}}, b_{\text{test}}\})V^*_{\text{prior}} \quad (6)$$

The value of information, *VI*, or the value obtained by performing an experiment, is defined, for an expected value maximize, as the expected profit given the test results minus the profit before testing as shown below

$$\begin{aligned} VI &= \text{expected profit after testing} - \text{expected profit before testing} \\ &= V_{\text{test}}\left\{\Omega_{\text{test}}, b_{\text{test}}\right\} - V^*_{\text{prior}} \\ &= P_{\text{stable}}\{\Omega_{\text{test}}, b_{\text{test}}\}V_{\text{stable}}\{\Omega_{\text{test}}, b_{\text{test}}\} \\ &\quad + (1 - P_{\text{stable}}\{\Omega_{\text{test}}, b_{\text{test}}\})V^*_{\text{prior}} - V^*_{\text{prior}} \\ &= P_{\text{stable}}\{\Omega_{\text{test}}, b_{\text{test}}\}V_{\text{stable}}\{\Omega_{\text{test}}, b_{\text{test}}\} - V^*_{\text{prior}} \end{aligned} \quad (7)$$

A test is only performed where the value of information is the highest. Therefore, the test parameters are selected using Eq. (8)

$$\begin{aligned} \{\Omega_{\text{test}}, b_{\text{test}}\} &= \max(VI) \\ &= \max\left(P_{\text{stable}}\{\Omega_{\text{test}}, b_{\text{test}}\}V_{\text{stable}}\{\Omega_{\text{test}}, b_{\text{test}}\} - V^*_{\text{prior}}\right) \end{aligned} \quad (8)$$

The expected value of the test is based on the prior probability of stability. After a test is performed, the prior cdf is updated using the test result. This updated posterior distribution is the prior distribution used to determine the next test point. This process is repeated for a selected number of tests. Once a stable result from a test is obtained (and for all further stable test results), V^*_{prior} is the maximum profit from all points known to be stable with certainty.

5 Experimental Results

Using the value of information approach, a sequence of 20 tests was completed. The operating conditions for each test point were selected to maximize the value of information at that time. Note that when using this value of information approach, each test is treated separately. For multiple tests, each test point is selected assuming that no additional tests will be completed. The random walk prior for this example was composed of 1×10^5 sample paths. Figure 12 shows the test points selected using the value of information approach, where stable test results are marked as "o" and unstable as "x". The results are also summarized in Table 2.

The stability was evaluated by observing the frequency content of the acceleration signal obtained by attaching a low-mass accelerometer to the flexure test platform, see Fig. 13. The sidewall surface was also used to identify unstable cuts. Figure 14 shows the frequency content of the acceleration signal and the machined surface for a test cut at {10,000 rpm, 6.25 mm}. For this stable result, content is observed only at the tooth passing frequency (166.66 Hz) and its harmonics and the surface is smooth. Figure 15 provides the same information for a cut at {8294 rpm, 8.34 mm}. Frequency content exists at frequencies other than the tooth passing frequency and its harmonics. Also, the surface has distinctive chatter marks indicating an unstable cut. Figure 16 shows the posterior stability cdf of stability after the 20 tests. Based on these results, the optimum operating point is {10,000 rpm, 6.25 mm} with a profit of $1206.50 per part.

To validate the performance of the algorithm, the analytical stability boundary was evaluated using a frequency-domain analytical approach [19]. The force model coefficients and the frequency response function (FRF) of the flexure on which the tests were performed were measured. The force model coefficients for the 6061-T6 workpiece material-tool combination were calculated using a linear regression to the mean values of *x* (feed) and *y* direction cutting forces measured over a range of feed per tooth values [19]. The FRFs of the flexure in the *x* (feed) and the *y*

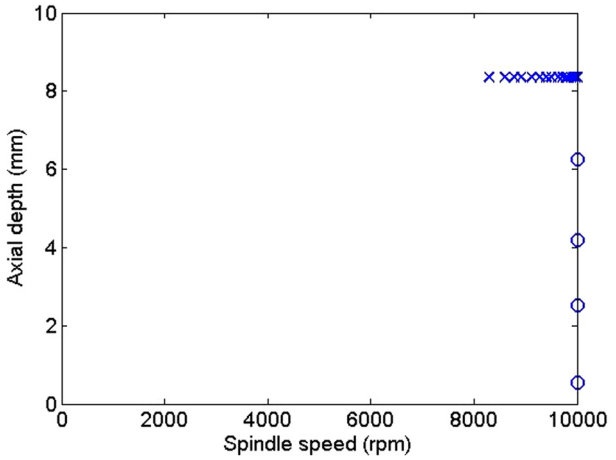

Fig. 12 Stability results for the value of information testing. The "o" symbols represent a stable result and the "x" symbols indicate an unstable result.

Table 2 Experimental test points and results

Test number	Spindle speed (rpm)	Axial depth (mm)	Stability result
1	10,000	0.54	Stable
2	10,000	2.51	Stable
3	10,000	4.18	Stable
4	10,000	6.25	Stable
5	10,000	8.36	Unstable
6	9819	8.36	Unstable
7	9639	8.36	Unstable
8	9920	8.36	Unstable
9	9398	8.36	Unstable
10	9117	8.36	Unstable
11	9719	8.36	Unstable
12	8916	8.36	Unstable
13	9960	8.36	Unstable
14	8595	8.36	Unstable
15	9498	8.36	Unstable
16	9880	8.36	Unstable
17	9278	8.36	Unstable
18	8294	8.36	Unstable
19	9779	8.36	Unstable
20	8776	8.36	Unstable

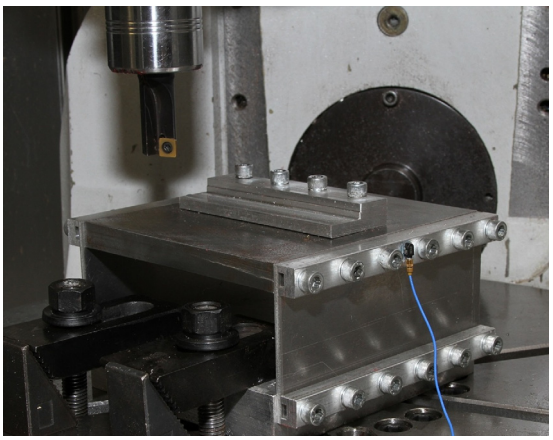

Fig. 13 Experimental setup for stability testing

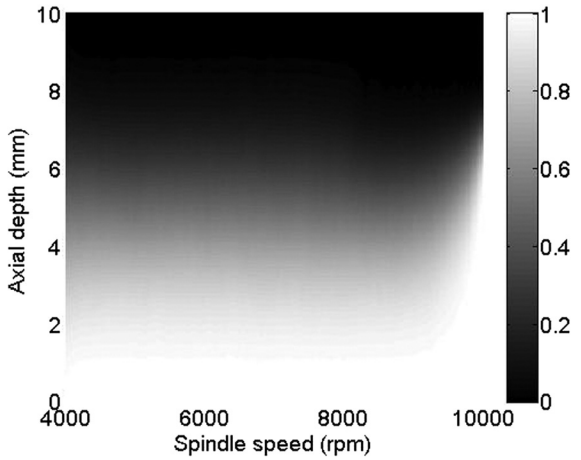

Fig. 16 Posterior stability cdf after 20 tests

directions were also measured using impact testing; see Fig. 17. The force coefficients are listed in Table 3. Figure 18 shows the stability lobes calculated along with the test points.

Note that from the analytical stability boundary, the optimum operating point is {7870 rpm, 8.34 mm} with a profit of $1220.00 per part. The operating point {10,000 rpm, 6.25}, which gives a profit of $1206.5, would not have been chosen based on the analytical boundary. However, the stability boundary obtained using the analytical is deterministic and uncertainty exists in the measured cutting force coefficients and FRFs, so some disagreement with experiment is anticipated. Even without knowledge of the system dynamics, the value of information approach was successful in locating the optimal operating point. The analytical stability lobes shown in Fig. 18 were also validated experimentally. Figure 19 shows the analytical prediction and the test results, where

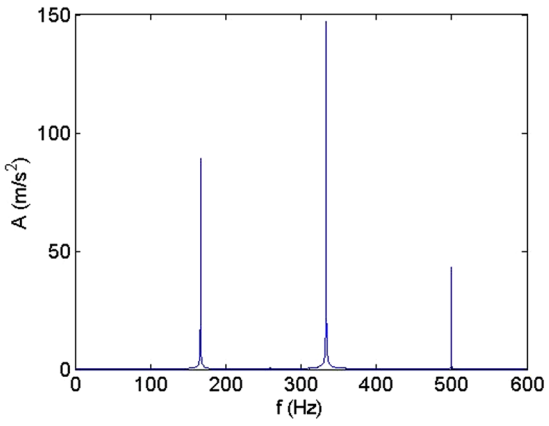

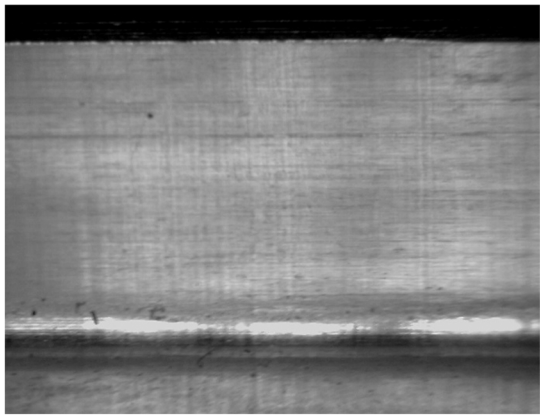

Fig. 14 Frequency content of the acceleration signal (left) and the machined surface (right) at {10,000 rpm, 6.25 mm}. Content is seen only at the tooth passing frequency (167 Hz) and its harmonics.

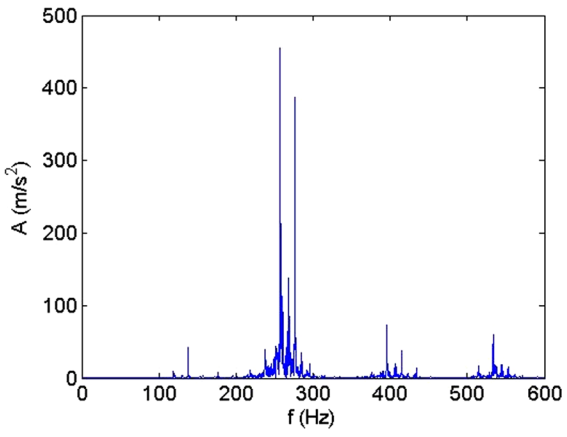

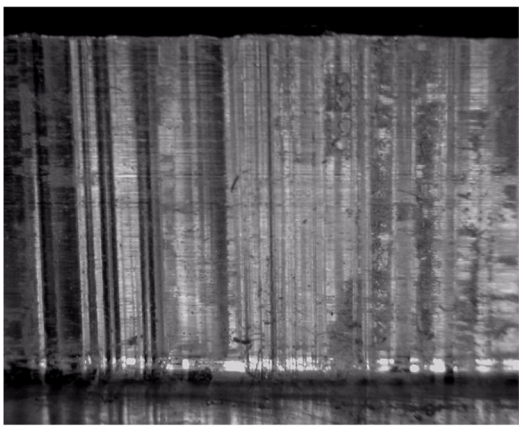

Fig. 15 Frequency content of the acceleration signal (left) and the machined surface (right) at {8294 rpm, 8.34 mm}. This unstable cut exhibits content other than tooth passing frequency and its harmonics (left) and chatter marks are observed (right).

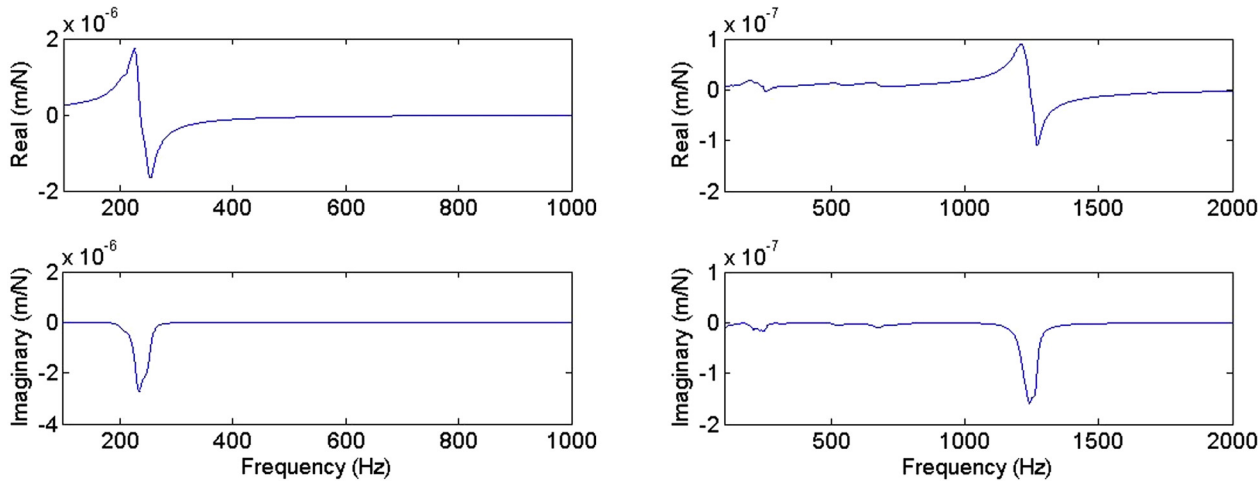

Fig. 17 FRFs for the flexure in the *x* (left) and the *y* (right) directions used in the experiments. Note that the dynamic stiffness is an order of magnitude higher in the *y* direction.

Table 3 Parameters used to determine the reference stability limit for the simulated testing scenario

Parameter	Value	Units
Tangential coefficient	853	N/mm^2
Normal coefficient	310	N/mm^2
Tangential edge coefficient	10.0	N/mm
Normal edge coefficient	8.0	N/mm

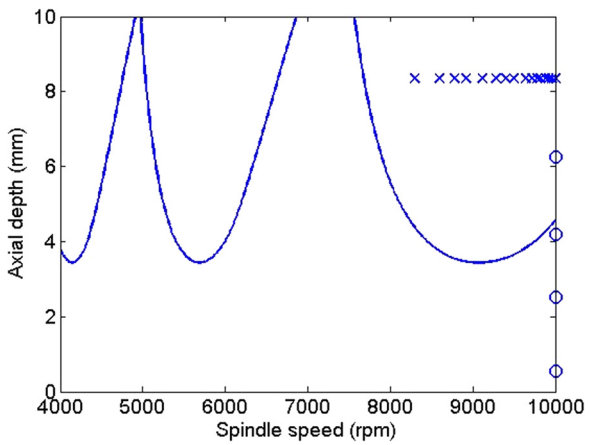

Fig. 18 Test point selections compared with the analytical stability lobes

"o" denotes a stable cut and "x" denotes an unstable cut. The testing locations were selected only to verify the lobe shape; the value of information approach was not applied.

6 Discussion

In this section, the effect of the standard deviation for the random walk step size on the posterior cdf and the test points is evaluated. The effect of the spindle speed-axial depth of cut domain on the posterior stability and test points is also explored.

Using the random walk approach, a test at any spindle speed updates the distribution at all spindle speeds. The extent to which a test at a spindle speed updates the distribution at spindle speeds other than the test speed depends on the standard deviation of the step size. To evaluate this dependence, random walks were generated using a normally distributed step size with zero mean and a standard deviation equal to 0.25 mm, $N(0,0.25)$. The random walks in Sec. 3 were generated using a standard deviation equal to 0.5 mm, $N(0,0.5)$. Consider that the updating was performed based on a stable test result at 7000 rpm and 5 mm. Figure 20 shows the updated cdf at 6500 rpm for both the standard deviations. As

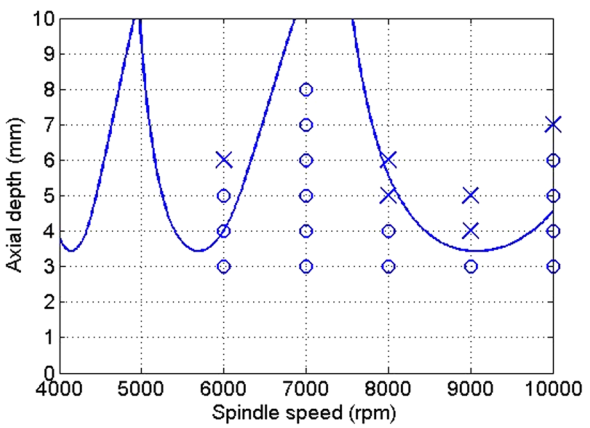

Fig. 19 Experimental validation of the stability lobes

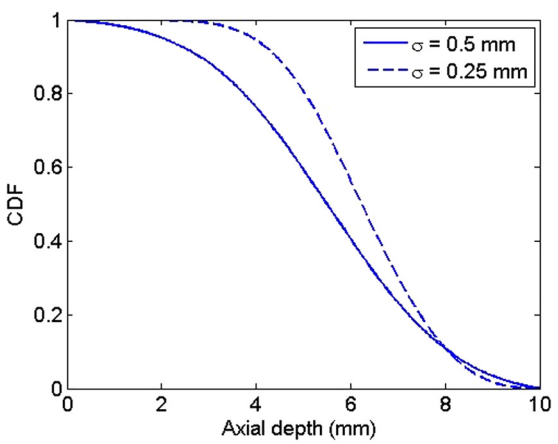

Fig. 20 The updated cdf at 6500 rpm given a stable test at {7000 rpm, 5 mm} with standard deviations of 0.5 mm and 0.25 mm for the random walk generation

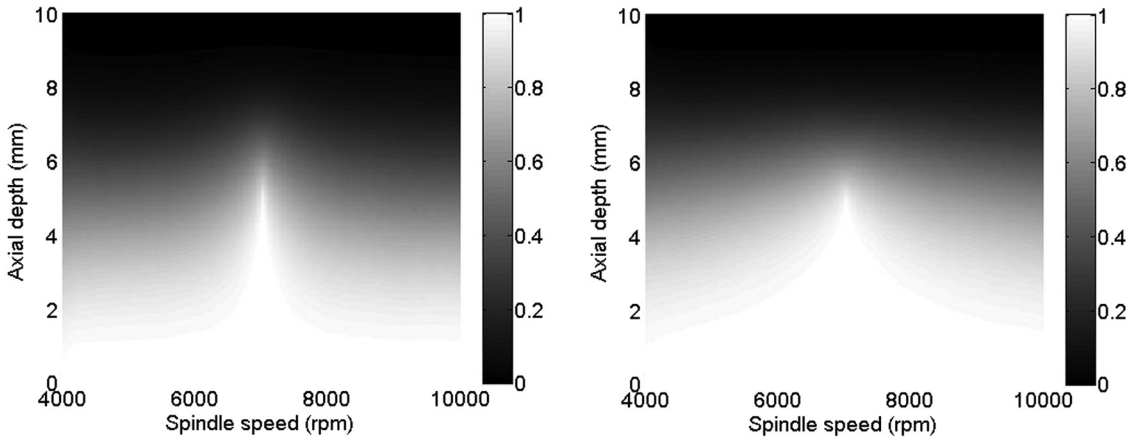

Fig. 21 Updated posterior cdf given a stable test result at {7000 rpm, 5 mm} for random walks generated using standard deviations of 0.5 mm (left) and 0.25 mm (right)

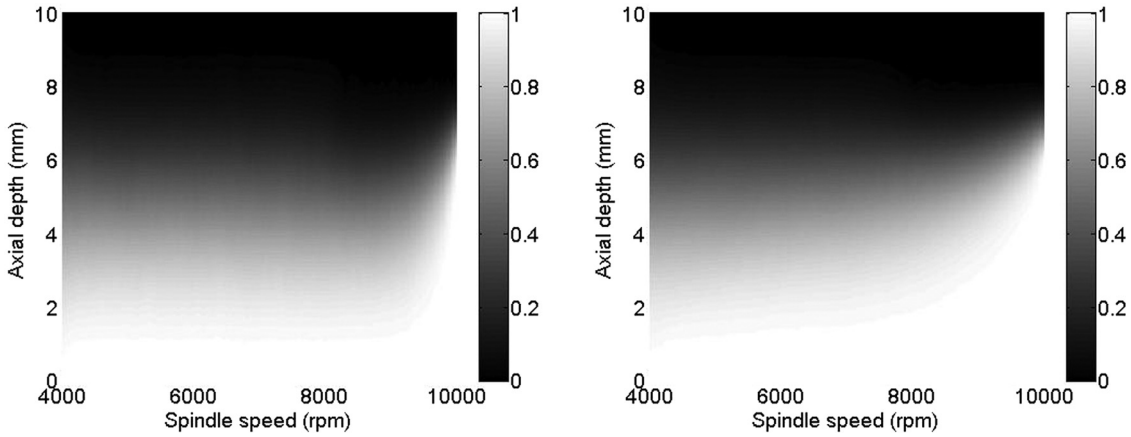

Fig. 22 Updated posterior cdf after 20 tests using random walks generated with standard deviations of 0.5 mm (left) and 0.25 mm (right)

Table 4 Experimental test points and results for spindle speed range of 4000 rpm to 8000 rpm

Test number	Spindle speed (rpm)	Axial depth (mm)	Stability result
1	8000	0.54	Stable
2	8000	5.01	Unstable
3	7197	5.01	Stable
4	7197	6.25	Stable
5	7250	8.36	Stable
6	7334	8.36	Stable
7	7571	8.36	Stable
8	7665	8.36	Stable

shown in the figure, the selected test does not affect the cdf at 6500 rpm for a standard deviation equal to 0.5 mm. The cdf is the same as the prior cdf as shown in Fig. 6. However, for the standard deviation of 0.25 mm, the cdf at 6500 rpm shows a probability of stability equal to unity at 2 mm. Figure 21 shows the updated posterior cdf given a stable test result at {7000 rpm, 5 mm} using random walks generated using a standard deviation of 0.5 mm (left) and 0.25 mm (right). The algorithm for selection of test points was repeated using the random walks generated with a standard deviation of 0.25 mm. Figure 22 shows a comparison of the updated posterior cdf after 20 tests for both cases. The algorithm converges to the same optimum operating point in both instances.

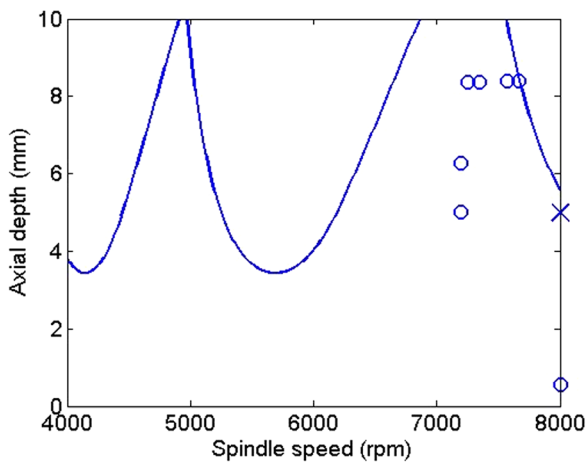

Fig. 23 Test point selection compared with the analytical stability lobes

A specific criterion for selecting the standard deviation of the step size is not presented here. However, trends have been observed. A higher standard deviation yields walks that are more volatile in the domain. This increases the number of remaining walks after each update (i.e., path filtering) using a test result and reduces the extent to which a test affects the cdf at all speeds in

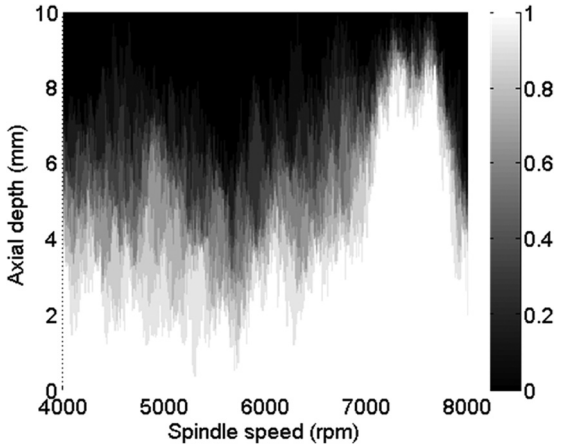

Fig. 24 Posterior cdf of stability after eight tests at a spindle speed range of 4000 rpm to 8000 rpm

the domain. As shown in Fig. 20, a standard deviation of 0.5 mm does increase the spread of the cdf at 6500 rpm given a stable test at {7000 rpm, 5 mm}. Therefore, a higher standard deviation provides a more conservative representation of the stability boundary.

The effect of the spindle speed-axial depth domain on the test point selection was also evaluated. The Bayesian updating procedure using random walks was repeated with a spindle speed domain from 4000 rpm to 8000 rpm. The test point selection was based on the value of information approach. Eight experiments were performed and the test result, stable or unstable, was determined based on the analytical stability lobe shown in Fig. 18. Table 4 shows the test points determined using the value of information approach. Figure 23 shows the test point selection and the analytical stability lobes; "o" represents a stable cut and "x" represents an unstable cut. Figure 24 shows the updated posterior cdf after eight tests. Using the value of information approach, the random walk method is robust and insensitive to the selected spindle speed-axial depth of cut domain. Although the nature of cdf is discrete, it does not affect the optimal operating point selection. Note that the optimal operating point was decided as the one which is known to be stable with certainty and the profit is the highest.

7 Conclusions

Bayesian inference using a random walk approach for stability prediction in milling was presented. The optimal test point selection was based on the value of information method. The motivation for implementing a Bayesian inference model was: (1) a Bayesian inference model enables a prediction which considers both theory and experimental results and (2) when using a Bayesian inference model, experiments can be chosen such that the expected value added by performing the experiment is maximized.

For the study presented here, no prior knowledge of the machining dynamics was assumed. Only stability test results were considered and the optimal experimental test point was selected using the value of information approach. Bayesian inference combined with decision analysis enables a dollar value to be placed on the information gained from an experiment prior to performing it. The stability updating was completed using random walks generated in the spindle speed-axial depth of cut domain, where the feature to be machined was selected to be a pocket. The value of information approach selects a test point which adds maximum value to profit taking into account the cost of machining the selected feature. The test points converged to the optimal operating point even without knowledge of the system dynamics. The proposed methodology enables a user to identify optimum stable machining parameters using stability experiments only without the knowledge of system dynamics. The approach is robust and insensitive to the spindle speed-axial depth of cut domain.

Acknowledgment

The authors gratefully acknowledge financial support for this work from the National Science Foundation (DMI-0642569 and DMI-0641827). They also wish to thank G. Hazelrigg for numerous helpful discussions.

References

[1] Tlusty, J., and Polacek, M., 1963, "The Stability of Machine Tools Against Self-Excited Vibrations in Machining," ASME Int. Res. Prod. Eng., **1**, pp. 465–474.
[2] Tobias, S. A., and Fishwick, W., 1958, *Theory of Regenerative Machine Tool Chatter*, The Engineer, London, **205**, p. 258.
[3] Merrit, H., 1965, "Theory of Self-Excited Machine Tool Chatter," ASME J. Eng. Ind., **87**(4), pp. 447–454.
[4] Arnold, R., 1946, "The Mechanism of Tool Vibration in the Cutting of Steel," Proc. Inst. Mech. Eng., **54**, pp. 261–284.
[5] Komanduri, R., 1993, "Machining and Grinding: A Historical Review of the Classical Papers," ASME Appl. Mech. Rev., **46**(3), pp. 80–132.
[6] Tlusty, J., 1978, "Analysis of the State of Research in Cutting Dynamics," Ann. CIRP, **27**(2), pp. 583–589.
[7] Smith, S., and Tlusty, J., 1991, "An Overview of Modeling and Simulation of the Milling Process," ASME J. Eng. Ind., **113**(2), pp. 169–175.
[8] Smith, S., and Tlusty, J., 1993, "Efficient Simulation Programs for Chatter in Milling," Ann. CIRP, **42**(1), pp. 463–466.
[9] Ehmann, K., Kapoor, S., DeVor, R., and Lazoglu, I., 1997, "Machining Process Modeling: A Review," ASME J. Manuf. Sci. Eng., **119**(4B), pp. 655–663.
[10] Smith, S., and Tlusty, J., 1997, "Current Trends in High-Speed Machining," ASME J. Manuf. Sci. Eng., **119**(4B), pp. 664–666.
[11] Merchant, M. E., 1998, "An Interpretive Look at 20th Century Research on Modeling of Machining," Mach. Sci. Technol., **2**(2), pp. 157–163.
[12] Altintas, Y., and Weck, M., 2004, "Chatter Stability of Metal Cutting and Grinding," Ann. CIRP, **53**(2), pp. 619–642.
[13] Kim, H. S., and Schmitz, T., 2007, "Bivariate Uncertainty Analysis for Impact Testing," Meas. Sci. Technol., **18**, pp. 3565–3571.
[14] Schmitz, T., and Duncan, G. S., 2005, "Three-Component Receptance Coupling Substructure Analysis for Tool Point Dynamics Prediction," ASME J. Manuf. Sci. Eng., **127**(4), pp. 781–790.
[15] Duncan, G. S., Kurdi, M., Schmitz, T., and Snyder, J., 2006, "Uncertainty Propagation for Selected Analytical Milling Stability Limit Analyses," Trans. NAMRI/SME, **34**, pp. 17–24.
[16] Mann, B. P., Bayly, P. V., Davies, M. A., and Halley, J. E., 2004, "Limit Cycles, Bifurcations, and Accuracy of the Milling Process," J. Sound Vib., **277**(2), pp. 31–48.
[17] Howard, R., 1966, "Information Value Theory," IEEE Trans. Syst. Sci. Cybern., **2**(1), pp. 22–26.
[18] Howard, R., 1970, "Decision Analysis: Perspectives on Inference, Decision and Experimentation," Proc. IEEE, **58**(5), pp. 632–643.
[19] Schmitz, T., and Smith, K., 2009, *Machining Dynamics: Frequency Response to Improved Productivity*, Springer, New York.